

FIBRE OPTICS

https://doi.org/10.1070/QEL17649

Investigation of performance properties of plastic optical fibres used in a traffic light system

S. Savović, A. Djordjevich, R. Min, I. Savović

Abstract. **We investigate the performance properties of a multimode plastic optical fibre (POF) used in a traffic light system. An analytical function is proposed for predicting the angular power distribution at the output end of a multimode optical fibre when the beam at the input end of the fibre is centrally launched along the fibre axis. We demonstrate how mode coupling affects the output angular power distribution along the fibre and, therefore, the performance of optical fibre used as part of a traffic light system. It is found that as the length of the POF increases, the angular power distribution broadens until it reaches a length at which a steady-state distribution (SSD) is achieved. This broadening is insignificant at short POF lengths of up to 10 m. As a result, the effective radiation area at the output end of any long POF as part of different light systems, such as traffic, building, and bridge light systems, can be determined.**

Keywords: *plastic optical fibre, mode coupling, power flow, traffic light system.*

1. Introduction

Plastic optical fibres (POFs) are made of low-cost plastics with visible transmission windows (500–800 nm), such as poly-(methyl-methacrylate) (PMMA), polystyrene, and polycarbonates. In comparison to silica optical fibres, which must be handled carefully and securely, POFs are much smoother and simpler to handle, with greater resistance to bending, shock, and vibration. POFs have now established themselves as a successful medium for short-range environments, where they provide the benefit of cost-effective deployment. POF networks have become very competitive in a variety of important applications for short-distance data communication, such as home networks, vehicle data connections, and industrial controls, thanks to technological advancements. POFs have also been commonly used for sensing, illumination, and lighting purposes due to their low cost, light weight, visible transmission window, and great flexibility.

The mode attenuation [1, 2] and rate of mode coupling [2–5] are both important factors in the transmission characteristics of plastic optical fibres. The latter is induced by fibre impurities and inhomogeneities introduced during the fibre manufacturing process (such as microscopic bends, irregularity of the core/cladding boundary and refractive index distribution fluctuations), and it results in power transfer between neighbouring modes. As compared to silica optical fibres, plastic optical fibres have much stronger mode coupling and greater mode attenuation [1, 2, 5–7].

The distribution of output angular power in the near and far fields of an optical fibre end has been extensively studied. Geometric optics (ray approximation) has been used to investigate mode coupling and predict output-field patterns [8, 9]. These patterns have been predicted as a function of the launch conditions and fibre length using the power flow equation [6, 7, 10–13], as well as the Fokker–Planck and Langevin equations [14]. The coupling coefficient D has been used to define the rate of mode coupling, which is the power transfer between modes [3, 11, 12, 15]. Modelling with this fibre parameter has been shown to correctly predict coupling effects observed in practice [see, for example, Refs 16, 17].

Although LED arrays and traffic lights have developed greatly, traffic lights are still not as safe as needed. When a LED array needs to be replaced or a traffic light needs repair, the traffic in one lane must be interrupted and lifts are needed to elevate the repairman, with all the danger that this involves, in addition to the economic cost and the traffic disruption caused. A new traffic light system with LED arrays at the base and a bundle of optical fibres to take the light to the top of the traffic light, to the disks, has been proposed [18]. The

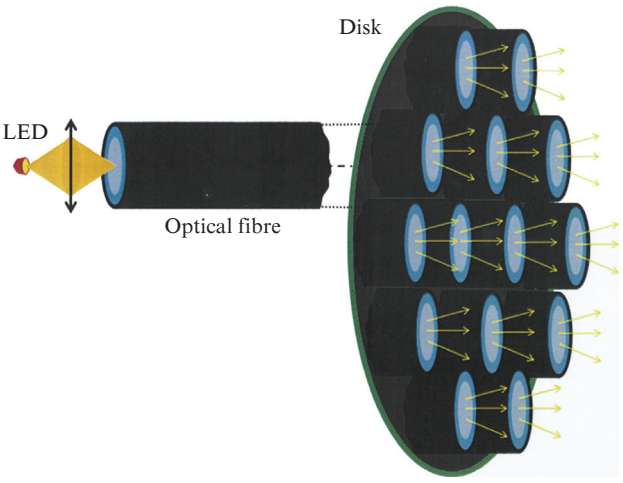

Figure 1. General scheme of a traffic light system [18].

S. Savović University of Kragujevac, Faculty of Science, R. Domanovića 12, 34000 Kragujevac, Serbia; e-mail: savovic@kg.ac.rs;
A. Djordjevich City University of Hong Kong, 83 Tat Chee Avenue, Kowloon, Hong Kong, China;
R. Min Center for Cognition and Neuroergonomics, Beijing Normal University at Zhuhai, China;
I. Savović University of Belgrade, 11000 Belgrade, Serbia

Received 30 July 2021
Kvantovaya Elektronika **51** (11) 1026–1029 (2021)
Submitted in English

traffic light is constructed in such a way that the optical fibre bundle which is connected to the illumination plate of the traffic light (Fig. 1) can be placed directly into the traffic light tube (Fig. 2), eliminating the need for modifications. We present numerical results for the evolution of mode power-distribution along the fibre with distance from the input fibre end for a POF used in Perez-Ocon et al.'s traffic light system [18], as well as how mode coupling affects the angular power distribution at the output fibre end. This is of interest in evaluating the effective radiation area at the output end of a fibre as part of the traffic light system.

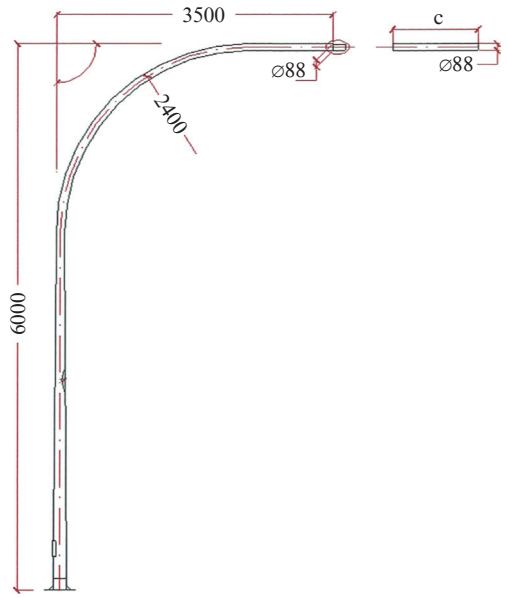

Figure 2. Model of a traffic light system (measurements in mm) [18].

2. Power flow equation

Gloge's power flow equation has the form [10]:

$$\frac{\partial P(\theta,z)}{\partial z} = -\alpha(\theta)P(\theta,z) + \frac{D}{\theta}\frac{\partial}{\partial\theta}\left(\theta\frac{\partial P(\theta,z)}{\partial\theta}\right), \tag{1}$$

where $P(\theta, z)$ is the output angular power distribution; z is the distance from the input end of the fibre; θ is the angle of propagation with respect to the core axis; D is the coupling coefficient assumed constant [6, 11]; and $\alpha(\theta)$ is the mode attenuation. The boundary conditions are set in the form $P(\theta_{cr}, z) = 0$, where θ_{cr} is the critical angle of the fibre, and $D(\partial P/\partial\theta) = 0$ at $\theta = 0$. The condition $P(\theta_{cr}, z) = 0$ denotes that modes with infinitely high loss do not hold power. The condition $D(\partial P/\partial\theta) = 0$ at $\theta = 0$ denotes that the coupling is restricted to the modes propagating with $\theta > 0$. Except near the cutoff region, attenuation is constant, $\alpha(\theta) = \alpha_0$, throughout the region of guided modes $0 \leqslant \theta \leqslant \theta_{cr}$ [11] [it occurs in the solution as the multiplication factor $\exp(-\alpha_0 z)$ which is independent of θ]. As a result, the dependence $\alpha(\theta)$ need not be accounted for when solving (1) for mode coupling, and this equation becomes [6, 12]:

$$\frac{\partial P(\theta,z)}{\partial z} = \frac{D}{\theta}\frac{\partial P(\theta,z)}{\partial\theta} + D\frac{\partial^2 P(\theta,z)}{\partial\theta^2}. \tag{2}$$

If the field distribution at the input end of the fibre is centred at $\theta_0 = 0$ [14] and the boundary condition $D(\partial P/\partial\theta) = 0$ is valid at $\theta = 0$, equation (2) is reduced to the form:

$$\frac{\partial P(\theta,z)}{\partial z} = D\frac{\partial^2 P(\theta,z)}{\partial\theta^2}. \tag{3}$$

The power distribution remains at the same angle with the distance from the input fibre end, but its width increases. If we consider $P(\theta, z)$ to be a probability distribution, equation (3) is then seen as the special Fokker–Planck equation with the constant diffusion coefficient D [14]. The solution of equation (3) is written in the form [19]:

$$P(\theta,z) = \frac{1}{\sqrt{2\pi}\,\sigma_z}\exp\left(-\frac{\theta^2}{2\sigma_z^2}\right). \tag{4}$$

The variance σ_z^2 of the output angular power distribution (4) at the fibre length z can be calculated as:

$$\sigma_z^2 = \sigma_{z=0}^2 + 2Dz, \tag{5}$$

where $\sigma_{z=0}^2$ is the variance of the input beam distribution. The coupling coefficient D from equation (5) is defined as [19]:

$$D = \frac{\sigma_z^2 - \sigma_{z=0}^2}{2z}. \tag{6}$$

Using equation (5), equation (4) now reads:

$$P(\theta,z) = \frac{1}{\sqrt{2\pi(\sigma_{z=0}^2 + 2Dz)}}\exp\left[\frac{\theta^2}{2(\sigma_{z=0}^2 + 2Dz)}\right]. \tag{7}$$

Taking attenuation into account, equation (7) can be written as:

$$P(\theta,z) = \frac{1}{\sqrt{2\pi(\sigma_{z=0}^2 + 2Dz)}}\exp\left[\frac{\theta^2}{2(\sigma_{z=0}^2 + 2Dz)}\right]\exp(-\alpha_0 z)\,. \tag{8}$$

Equation (8) describes spatial transients of the power distribution along a multimode SI optical fibre of z length when the power distribution at the input end of the fibre is centred at $\theta_0 = 0$ with standard deviation $\sigma_{z=0}$. To the best of our knowledge, we propose for the first time an analytical function (8) for predicting the angular power distribution at the output end of a multimode optical fibre when the beam at the input end of the fibre is centrally launched along the fibre axis, which is the most common case in the practical employment of a multimode optical fibres. Compared to our earlier proposed analytical function (4), which considers only mode coupling coefficient D, function (8) takes into account the attenuation constant α_0 as well.

3. Numerical results and discussion

We investigated spatial power distribution transients in a multimode SI POF used in a recently proposed traffic light system [18]. The optical fibre was a TORAY PGU-CD1001-22E with a PMMA core and fluorinated polymer cladding. The core refractive index was $n_1 = 1.492$, the fibre diameter was $b = 1.0$ mm, NA = 0.5, and the attenuation was $\alpha_0 = 0.15$ dB m^{-1}. The fibre was illuminated with a Hebei I.T. 520PG0C LED with $\sigma_{z=0} = 9°$ (Fig. 3) [18]. Perez-Ocon et al. [18] obtained the normalised experimental output angular power distribution for an LED light beam launched centrally

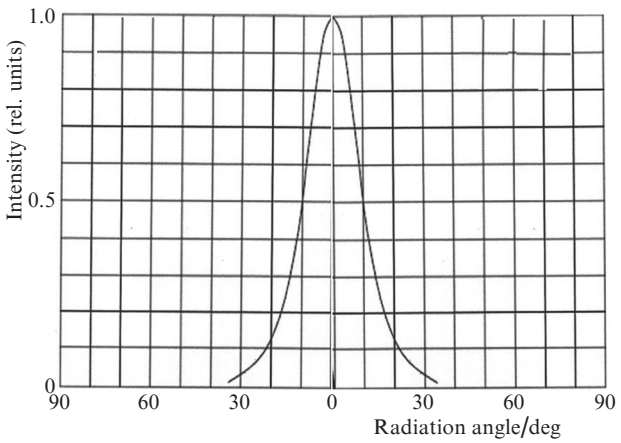

Figure 3. Relative intensity as a function of radiation angle of LED (Hebei I.T.520PG0C) [18].

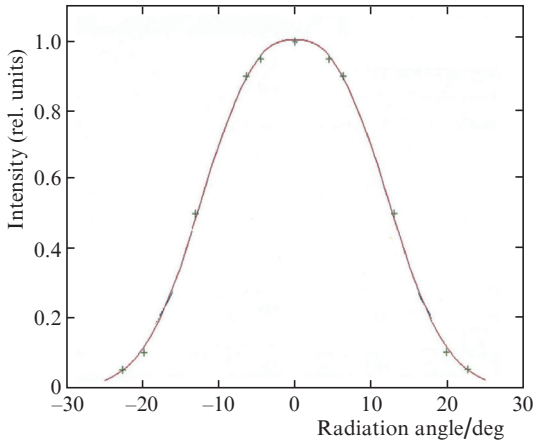

Figure 4. Experimental relative intensity as a function of radiation angle measured at the output fibre end for a LED beam launched centrally along the fibre axis [18].

($\theta_0 = 0$) along the fibre axis (the fibre length was 10 m), with the standard deviation of the experimental output angular power distribution of $\sigma_z = 11.5°$ (Fig. 4). Introducing these values into equation (6), we obtained the coupling coefficient $D = 7.8 \times 10^{-4}$ rad^2 m^{-1}.

To make it easier to compare the results, we use the calculated coupling coefficient D to solve the power flow equation (2), which gives us the coupling length L_{coup} at which the equilibrium mode distribution (EMD) is achieved, as well as the length z_s at which the SSD is established, in the fibre used in the experiment by Perez-Ocon et al. [18]. We obtained the output angular power distribution for different launch angles at various fibre lengths by using the explicit finite difference method [12] to solve the power flow equation (2), as shown in Fig. 5. We show the results for four input angles $\theta_0 = 0$, 8° and 16° measured inside the fibre ($\theta_0 = 0$, 12° and 24.3° measured in air). Input angles near the critical angle $\theta_{cr} = 18.9°$ measured inside the fibre ($\theta_{cr} = 28.8°$ measured in air) have not been included because the attenuation constant $\alpha(\theta)$ cannot be neglected near the critical angle when solving the original power flow equation (1).

We chose a Gaussian launch-beam distribution with $\sigma_{z=0} = 9°$ {the same $\sigma_{z=0}$ was used in Perez-Ocon et al.'s experiment [18] (Fig. 3)}. The fibre length z was increased from zero to achieve the SSD. Because of mode coupling, all mode dis-

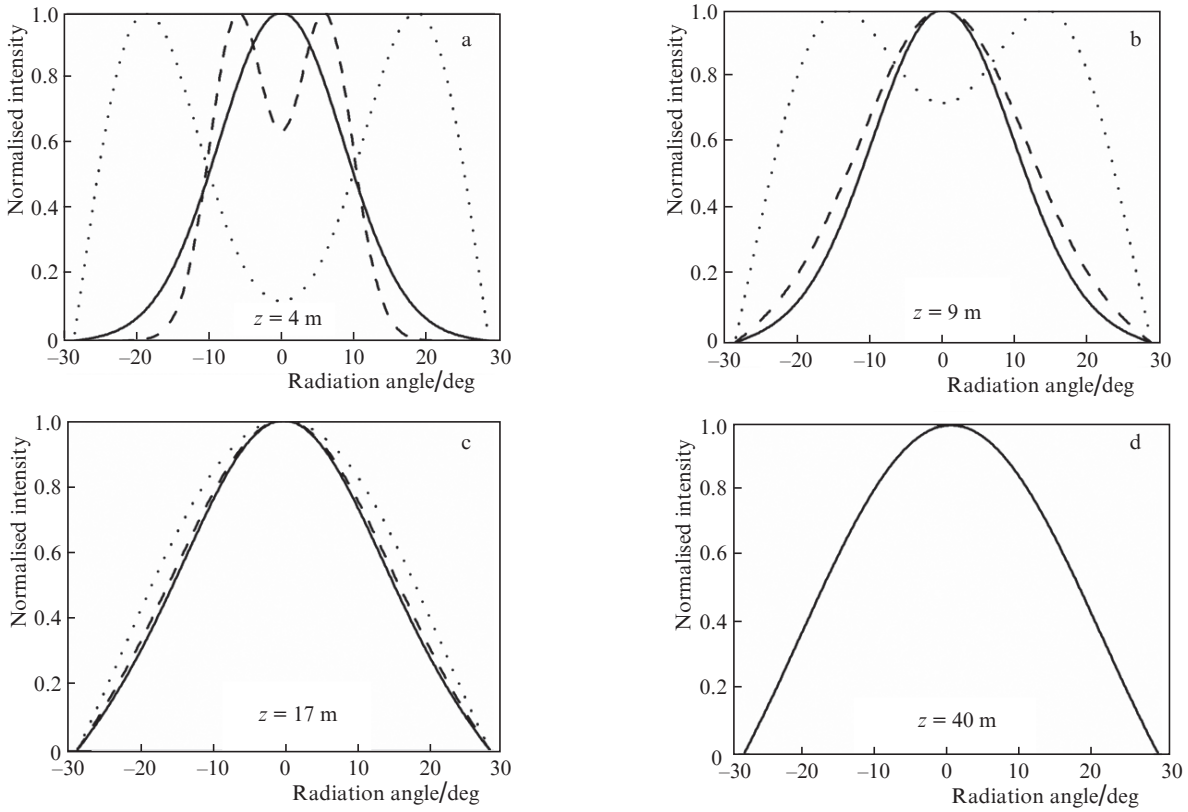

Figure 5. Normalised output angular power distribution at different locations along SI POF calculated for Gaussian input angles θ_0 = (solid curve) 0, (dashed curve) 12°, and (dotted curve) 24.3° measured in air with $\sigma_{z=0} = 9°$ for z = (a) 4, (b) 9, (c) 17 and (d) 40 m.

tributions shifted their midpoints to 0, resulting in the EMD at fibre length L_{coup} = 17 m (Fig. 5c). The coupling continues beyond the L_{coup} mark on the fibre until all distribution widths equalise and a SSD is reached at z_s = 40 m (Fig. 5d). There is no further broadening of the angular power distribution at lengths $z > z_s$. As part of a proposed traffic light system [18], we determine in this way an effective radiation area at the output end of an arbitrary long POF. Such results can be used for optimisation of the number of fibres, their mutual distance and positions at the traffic light disk.

To conclude, a fibre with a sufficient length should be used in order to realise a larger effective radiation area, ideally fibre with length $z > z_s$, at which relative energy packet population in each mode no longer changes with propagation length. Such a long fibre length is common in POF employment in building and bridge light structures. One should note that in the case that optical fibre is installed with sharper bends with radius $r \leqslant 0.30$ m [20] compared to the bend with radius of r = 2.5 m [18], in the calculation of the angular power distribution one should employ different mode coupling coefficient for bent fibre sections.

4. Conclusions

We have investigated how the angular power distribution in a multimode plastic optical fibre used in a traffic light system changes as the fibre length increases. In order to achieve this goal, we have proposed an analytical function for predicting the angular power distribution at the output end of a multimode optical fibre when the beam at the input end of the fibre is centrally launched along the fibre axis. We have found that as fibre length increases, the angular power distribution broadens until it reaches a steady-state distribution. This broadening is negligible at short fibre lengths of up to about 10 m. This method can be used to calculate the effective radiation area at the output end of any arbitrary long POF. A fibre with a sufficient length should be used in order to realise a larger effective radiation area. This information is useful for the use of multimode POFs as part of traffic, building, and bridge light systems.

Acknowledgements. This research was made possible in part by a grant from the Serbian Ministry of Education, Science, and Technological Development (Agreement No. 451-03-68/2020-14/200122), by the grant from Science Fund of Republic Serbia (Agreement No. CTPCF-6379382) and by the Strategic Research Grant of City University of Hong Kong (Project No. CityU 7004600).

References

1. Kitayama K., Ikeda M. *Appl. Opt.*, **17**, 3979 (1978).
2. Mateo J., Losada M.A., Garcés I., Zubía J. *Opt. Express*, **14**, 9028 (2006).
3. Dugas J., Maurel G. *Appl. Opt.*, **31**, 5069 (1992).
4. Jiang G., Shi R.F., Garito F. *IEEE Photonics Technol. Lett.*, **9**, 1128 (1997).
5. Garito A.F., Wang J., Gao R. *Science*, **281**, 962 (1998).
6. Gambling W.A., Payne D.P., Matsumura H. *Appl. Opt.*, **14**, 1538 (1975).
7. Zubía J., Durana G., Aldabaldetreku G., Arrue J., Losada M.A., Lopez-Higuera M. *J. Lightwave Technol.*, **21**, 776 (2003).
8. Eve M., Hannay J.H. *Opt. Quantum Electron.*, **8**, 503 (1976).
9. Arrue J., Aldabaldetreku G., Durana G., Zubía J., Garcés I., Jiménez F. *J. Lightwave Technol.*, **23**, 1253 (2005).
10. Gloge D. *Bell Syst. Tech. J.*, **51**, 1767 (1972).
11. Rousseau M., Jeunhomme L. *IEEE Trans. Microwave Theory Tech.*, **25**, 577 (1977).
12. Djordjevich A., Savović S. *IEEE Photonics Technol. Lett.*, **12**, 1489 (2000).
13. Savović S., Djordjevich A. *Appl. Opt.*, **41**, 7588 (2002).
14. Savović S., Djordjevich A. *Appl. Opt.*, **41**, 2826 (2002).
15. Jeunhomme L., Fraise M., Pocholle J.P. *Appl. Opt.*, **15**, 3040 (1976).
16. Losada M.A., Mateo J., Garcés I., Zubía J.. Casao J.A., Peréz-Vela P. *IEEE Photonics Technol. Lett.*, **16**, 1513 (2004).
17. Losada M.A., Garcés I., Mateo J., Salinas I., Lou J., Zubía J. *J. Lightwave Technol.*, **20**, 1160 (2002).
18. Pérez-Ocón F., Pozo A.M., Rubiño M., Rabaza O. *Eng. Struct.*, **96**, 1 (2015).
19. Savović S., Djordjevich A. *Appl. Opt.*, **46**, 1477 (2007).
20. Savović S., Djordjevich A. *Appl. Opt.*, **47**, 4935 (2008).